PDA-cross-linked beta-cyclodextrin: a novel adsorbent for the removal of BPA and cationic dyes

Jianyu Wang, Guang Cheng, Jian Lu, Huafeng Chen and Yanbo Zhou IWA

ABSTRACT

In this study, 4,4′-(hexafluoroisopropene) diphthalic acid (PDA)-CD polymers containing β-cyclodextrin (CD) were synthesized for the adsorption of endocrine disrupting chemicals (EDCs) and dyes. It features great adsorption of bisphenol A (BPA), methylene blue (MB) and neutral red (NR). The maximum adsorption capacities of MB, NR and BPA can reach 113.06, 106.8 and 51.74 mg/g, respectively. The tandem adsorption results revealed that adsorptions of dyes and BPA onto PDA-CD polymer were two independent processes: non-polar BPA entrapment by cyclodextrin cavities while dyes were captured by the carboxyl groups and π-π stacking interactions. The adsorption processes performed well in a wide range of pH (4.0–10.0) and were not affected by fulvic acid (FA) and inorganic ions.

Key words | adsorption, bisphenol A, cyclodextrin, dyes, polymer adsorbent

Jianyu Wang
Guang Cheng
Jian Lu
Huafeng Chen
Yanbo Zhou IWA (corresponding author)
National Engineering Laboratory for Industrial Wastewater Treatment,
East China University of Science and Technology,
No. 130 Meilong Road, Shanghai 200237,
China
E-mail: *zhouyanbo@ecust.edu.cn*

Yanbo Zhou
State Environmental Protection Key Laboratory of Environmental Risk Assessment and Control on Chemical Process,
East China University of Science and Technology,
No. 130 Meilong Road, Shanghai 200237,
China

HIGHLIGHTS

- PDA-CD with abundant cavities, benzene rings and carboxyl groups were successfully fabricated.
- PDA-CD showed excellent adsorption capacity for dye and BPA.
- The molecular recognition by CD cavity contributed to the BPA adsorption.
- Electrostatic attraction and π-π interaction dominated dye adsorption.

GRAPHICAL ABSTRACT

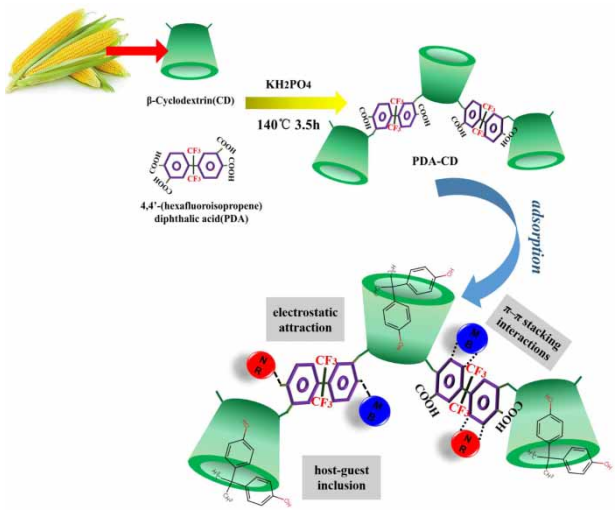

doi: 10.2166/wst.2020.286

INTRODUCTION

In the textile industry, large volumes of water and chemicals are required in processing. According to statistics, about 200 L of water is consumed to manufacture 1 kg of textile (Zhou *et al.* 2019b). More than 100,000 commercially available dyes with approximately 7,000 hundred tons of dyestuff are synthesized each year (Robinson *et al.* 2001). The discharge of textile wastewaters into water bodies normally affects the aquatic organisms and human beings (Verma *et al.* 2012; Liu *et al.* 2020). Conventional efficient methods of removing dyes mainly include adsorption technology (Gamoudi & Srasra 2019; Kloster *et al.* 2019), advanced oxidation (Van *et al.* 2019; Yang *et al.* 2019) and membrane separation (Guo *et al.* 2019; Konca & Çulfaz-Emecen 2019). Normally, the main deficiencies in membrane separation technology consist of high cost, frequent membrane fouling and requirement for different pretreatments (Verma *et al.* 2012). Intermediates with high toxicity may occur during the advanced oxidation processes and effectiveness fluctuates widely with the type of pollutants present in the textile wastewater (Verma *et al.* 2012). Adsorption technology has become an extensive approach to remove dyes as it is cost-effective, offers easy operation and is highly efficient (Qadeer 2007). However, many people just pay attention to dye removal from textile wastewater and ignore endocrine disrupting chemicals (EDCs) in effluents (Zhou *et al.* 2019b). Bisphenol A (BPA) is used as an intermediate chemical in the manufacture of antioxidants and dyes (Xue *et al.* 2017). Excessive BPA from textile wastes has been detected (Zijian *et al.* 2015). BPA is a very typical EDC and important raw material for polycarbonate plastics and resins. Thus, the removal of coexisting pollutants in textile effluents becomes a matter of continuing concern.

Recently, use of by-products from agricultural and forestry waste as raw materials to prepare green adsorbents has become a hot topic in the environmental field because of their non-toxicity and easy access (Ozmen *et al.* 2008). β-cyclodextrin (CD) is a kind of oligosaccharide extracted from starch-containing crops by catalytic enzymes. CD-based materials have been widely used to remove dyes, organic matters, metal ions and active bacteria from water (Chen *et al.* 2020; Hu *et al.* 2020). The development trend of CD materials is to construct porous materials with high specific surface area and high porosity to absorb or degrade micropollutants in water (Zhou *et al.* 2020). The uniqueness of CD lies in its spatial structure. The nature of a hydrophobic cavity at the center of molecular CD allows the formation of a host-guest inclusion complex with guest compounds through a hydrophobic-hydrophobic interaction (Choi *et al.* 2019; Xu *et al.* 2020). It is noteworthy that the high density of oxhydryl groups on the exterior are given a great chance to be modified by diverse functional groups, furnishing the CD with extra specific properties, which makes it possible for it to become an adsorption material. But being a high water-soluble cyclodextrin monomer unavoidably limited its application in the field of adsorption. Thus, water-insoluble cyclodextrin polymers have been widely researched by many people (Crini 2014; Wu *et al.* 2018). A cross-linking agent rich in carboxylic acid, such as citric acid (Huang *et al.* 2018), thiomalic acid (Zhang *et al.* 2019) and EDTA (Zhao *et al.* 2015), has always been the first choice because the carboxyl groups not only perform as cross-linking sites, but also as adsorption sites. And the process is usually handy to operate.

A 4,4′-(hexafluoroisopropene) diphthalic acid (PDA) molecule contains two benzene rings and four carboxyl groups. The ample carboxyl groups can be cross-linked with the hydroxyl groups of the cyclodextrin to form a water-insoluble polymer. In theory, the carboxyl groups and hydrophobic cavity can provide adsorption sites for cationic dyes and BPA, respectively. When organic pollutants with hydrophobic parts or phenyl groups and nitrogen cations are absorbed, people have not figured out whether the hydrophobic cavity and surface groups interfere with each other. Fortunately, based on previous researches (Zhao *et al.* 2009; Liu *et al.* 2015), we can conjecture that while CD comes across an amphiphilic guest molecule, its cavity inclines to mastery of the hydrophobic part of the molecule, and the remaining part will interact with the polar groups on the surface (Huang *et al.* 2018).

In this paper, an insoluble water PDA-CD was successfully prepared with a carboxyhydroxy esterification crosslinking principle. The use of PDA as a crosslinking agent has the following advantages: (1) rich carboxyl groups can provide more adsorption sites for cationic dyes (Chen *et al.* 2020); (2) benzene rings of PDA can form a conjugation effect with benzene rings in dyes; (3) the preparation process is simple and convenient. The morphological structure of PDA-CD was analyzed. Cationic dyes such as methylene blue (MB) and neutral red (NR), and BPA were used as target pollutants to further study the adsorption performance. The effects of initial pH of the solution, fulvic acid (FA) and inorganic ions on the adsorption performance were studied.

MATERIALS AND METHOD

Materials

4,4′-(hexafluoroisopropene) diphthalic acid (PDA), β-cyclodextrin (CD), bisphenol A (BPA), methylene blue (MB) and neutral red (NR) were purchased from Aladdin Industrial (China). Fulvic acid (FA) was bought from Shanghai Yuanye Bio-Technology (China). KCl and $CaCl_2$ were obtained from Shanghai Lingfeng Chemical Reagent (China). All the chemicals were 98 + % pure. Other chemical agents used in this paper were analytical reagent grade. Water used in this paper was purified using a Milli-Q water purification system from Millipore (USA). All reagents were used without further purification.

Preparation of PDA-CD

In the process of synthesis (Figure 1), potassium dihydrogen phosphate, PDA and CD acted as catalyst, crosslinking agent and matrix, respectively. The active hydroxyl group on CD was esterified with a polyvalent carboxyl group on PDA. The cross-linking reaction is carried out to crosslink a plurality of cyclodextrin monomers together to obtain water-insoluble PDA-CD polymers. According to different molar ratios (PDA: CD = 3:1, PDA: CD = 4:1, PDA: CD = 5:1), an accurately weighed certain amount of β-CD and PDA were added into a 600 mL beaker. The sum of the mass of CD and PDA in the three molar ratios was 1.5 g, and 0.25 g of potassium dihydrogen phosphate (KH_2PO_4) was added to each beaker. 100 mL of deionized water was used to solubilize the material in the beaker. Then, the beaker was placed in an oven and reacted at 140 °C for 3.5 h. After the reaction was completed, the materials were repeatedly rinsed with deionized water to remove surface residue of the materials, and the washed materials were placed in an oven to be dried to constant weight.

Characterization and adsorption performance test

All PDA-CD polymers were dried prior to inspection to avoid the effect of moisture on the characterization of the materials. Scanning electron microscopy (SEM) measurements were employed with a Hitachi S-3400N scanning electron microscope. Fourier transform infrared (FT-IR) spectra were recorded to distinguish the functional groups of polymers via a Nicolet 5700 spectrometer. The specific surface area of the polymers was calculated using the Brunauer Emmett Teller (BET) method with a Micromeritics TriStar II 3020 surface area and porosity analyzer.

In this paper, three pollutants, MB, NR and BPA were selected as target pollutants. FA, widely used to represent other organics in water, reflects the influence of organics for adsorbents (Yang & Xing 2009).Three different molar ratios of PDA-CD polymers were explored. The removal efficiency was calculated by Equation (1). Three parallel experiments were performed on the same pollutants and pH conditions, and the average value was taken as the final result.

$$\text{Removal efficiency } (\%) = \frac{(C_0 - C_e)}{C_0} \times 100\% \quad (1)$$

where C_0 (mg/L) and C_e (mg/L) represent the initial pollutants concentration and equilibrium concentration of pollutants.

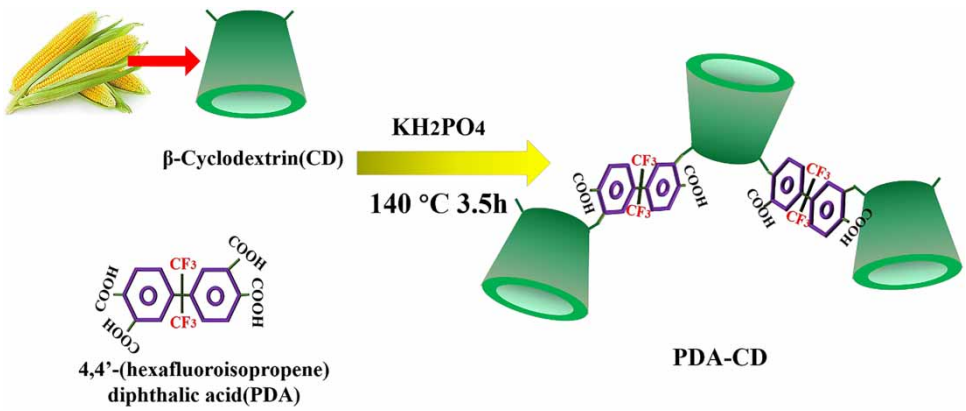

Figure 1 | Fabricating of PDA-CD polymers.

Effect of pH

Zeta potentials under different pH values of solution were obtained at 25 °C using Zeta sizer Nano ZS (Malvern ZEN3600). The capacity of adsorption was estimated by removal efficiency of pollutants. During the experiment, the initial concentration of the three target pollutant solutions was set to 50 mg/L, and the pH values range of the MB and BPA solutions was set from 2.0 to 10.0. Since NR is an acid-based indicator, it features different colors under different acid-based conditions, which is not conducive to detection. At the same time, it was found that NR solution will produce flocculent precipitation under alkaline conditions, influencing the accuracy of the test results. So the pH values range of the NR solution was set from 2.0 to 6.0. The pH of the solutions was adjusted with HCl and NaOH.

Adsorption isotherms

Different concentrations of pollutants (MB and NR: 10–500 mg/L, 50 mL; BPA: 5–200 mg/L, 50 mL) were prepared in a 150 mL erlenmeyer flask. 50 mg PDA-CD polymers were added into each flask. For better studying the adsorption mechanism between pollutants and polymers, three adsorption isotherm models were selected to fit the experimental data, namely Langmuir, Freundlich and Sips models.

Equation (2) is the calculation formula of the Langmuir model (Chen *et al.* 2019).

$$q_e = \frac{K_L q_m C_e}{1+K_L C_e} \tag{2}$$

In the formula, C_e (mg/L) represents the equilibrium concentration of contaminants; q_e (mg/g) and q_m (mg/g) represent equilibrium as well as theoretical saturated adsorption capacity, respectively; K_L represents the Langmuir isotherm constant with respect to enthalpy and adsorption energy and its unit is L/mg.

Equation (3) is the calculation formula of the Freundlich model.

$$q_e = K_F C_e^{1/n_f} \tag{3}$$

In the formula, K_F ((mg/g) $(L/mg)^{nf}$) represents the Freundlich capacity constant, indicating the magnitude of the adsorption capacity; $1/n_f$ is the heterogeneity factor (Raza *et al.* 2019).

Equation (4) is the calculation formula of the Sips model.

$$q_e = \frac{q_m (K_S C_e)^{1/n_s}}{1 + (K_S C_e)^{1/n_s}} \tag{4}$$

In the formula, K_S (L/mg) and n_s^{-1} represents the Langmuir association constant and the Freundlich heterogeneity parameter, respectively.

Adsorption kinetics

The 0.1 g PDA-CD were respectively added into 100 mL of MB, NR and BPA solution (pollutant concentration: 50 mg/L), stirring for one hour (250 rpm/min). Water samples were achieved at predefined time intervals (0, 5, 10, 20, 30, 40, 60, 120, 180 min). The adsorption capacity q_t of the adsorbent at different time points is calculated by Equation (5).

$$q_t = \frac{(C_0 - C_t)V}{m} \tag{5}$$

where C_0 (mg/L) and C_t (mg/L) represent the initial and residual the concentration of the pollutants, whereas V (mL) represents the volume of the pollutant solution and m (mg) means to the total mass of the adsorbent.

All experimental data were fitted with non-linearized pseudo-second-order kinetic model (Acemioglu 2005) as calculated as Equation (6).

$$q_t = \frac{K\, q_e^2 t}{(1 + K\, q_e t)} \tag{6}$$

where K (g/mg/min) and q_e (mg/g) represent the pseudo-secondary adsorption kinetic constants and the equilibrium adsorption capacity at a reaction time of t, respectively.

Tandem adsorption

According to the adsorption sequences of these three pollutants, the experiments have been divided into two forms: dual (NR/MB, BPA/MB, MB/NR, BPA/NR, NR/BPA, MB/BPA) and triple (NR/BPA/MB, BPA/NR/MB, MB/BPA/NR, BPA/MB/NR, MB/NR/BPA, NR/MB/BPA). Different forms of systems represent different adsorption sequences; for instance, NR/MB means adsorption of MB after the completion of NR adsorption. Specifically, the 0.1 g PDA-CD were added into 100 mL of NR solution

(concentration: 50 mg/L), stirring for three hours (250 rpm/min), and concentration of pollutants were measured at the designed intervals (0, 5, 10, 20, 30, 40, 60, 120, 180 min). After 3 h, the adsorbed NR PDA-CD were separated from solution and added into MB solution (concentration: 50 mg/L) to carry on adsorption again. Furthermore, NR/MB/BPA expresses adsorption of BPA after the completion of the NR/MB adsorption. Specifically, the polymers adsorbed on NR and MB were separated from solution and added to a solution of 100 mL of BPA at a concentration of 50 mg/L. Physical and chemical conditions and sampling conditions were the same in all adsorption processes.

Effect of fulvic acid and inorganic ion

Effect of fulvic acid

50 mL (MB: 50 mg/L, NR: 50 mg/L; BPA: 50 mg/L) solutions were prepared respectively in a 150 mL erlenmeyer flask and appropriate amount of humic acid were added to each flask. The concentrations of humic acid in the solutions were designed as 20, 50, 100 and 200 mg/L respectively, and a blank experimental group was set as a control. The dosage of the polymers was set as 1 g/L. The conical flasks were shaken for 24 h at 25 °C. After the oscillating adsorption, the precipitate processes were completely allowed to stand for 30 min, and the supernatant in the conical flasks were taken for detection.

Effect of inorganic ion

The presence of inorganic ions may affect the adsorption performance of polymers in water. Therefore two kinds of inorganic ions (K^+&Ca^{2+}) have been selected to study the adsorption properties of adsorbent PDA-CD on the three pollutants in the presence of inorganic ions in solution. 50 mL (MB: 50 mg/L, NR: 50 mg/L, BPA: 50 mg/L) solutions were prepared respectively in 150 mL erlenmeyer flasks. K^+ and Ca^{2+} were provided by potassium chloride and calcium chloride, respectively. The concentrations of potassium and calcium ions in each kind of pollutant solution were both set as 20 mg/L and 200 mg/L, along with a blank experimental group as a control.

Analytical method of pollutant concentration

The BPA involved in this paper was detected by L-2000 high performance liquid chromatography. The column of the instrument was a C18 column of Guoan Jielun Company (4.6 × 250 mm, 2.5 μm), the mobile phase used methanol and water (70/30, v/v), the column temperature was controlled at 40 °C, and the UV detection wavelength was 278 nm. All test samples should be filtered using a 0.22 μm hydrophilic Teflon needle filter to protect the column before testing. The concentrations of MB and NR, were tested using a Unico 2802 UV-Vis spectrophotometer. According to the full wavelength scanning of the two dye ions, the maximum absorption wavelengths of MB and NR are 665 nm and 530 nm, respectively. All the experimental data in this paper were obtained by three repeated parallel experiments, and the difference between the obtained data was analyzed.

RESULT AND DISCUSSION

Characterizations and properties of PDA-CD

The FT-IR spectra of the three different molar ratios of PDA-CD and original materials (PDA and CD) are illustrated in Figure 2(d). The CD and PDA-CD of three different molar ratios all exhibited strong absorption peaks with a large span in the range of 3,000 cm^{-1} to 3,700 cm^{-1}, resulting from stretching vibrations of -OH in β-ring. PDA-CD in three ratios all exhibited new strong absorption peaks at 1,737 cm^{-1}, associated with stretching of C = O groups from carboxyl groups. Beyond that, PDA-CD all presented two new absorption peaks at 1,149 cm^{-1} and 1,027 cm^{-1}, ascribing to -COC- and CO stretching vibrations of structure of CD (Chen *et al.* 2020) and revealed fluorine related peaks in the range from 1,214 cm^{-1} to 1,251 cm^{-1} (Ren *et al.* 2004). These results demonstrate the success of CD and PDA crosslinking esterification. For studying the surface morphology and pore structure characteristics of CD polymer, three ratios of polymers were scanned by SEM and BET analysis. The SEM and BET of three molar ratios of synthesis are displayed in Figure 2(a)–2(c). As the proportion of the cross-linking agent PDA in the CD polymer decreased, the surface of the prepared polymers gradually approached smoothness, the crumb-like substances gradually decreased, and cracks appeared. The BET values of three different molar ratios of PDA-CD polymers (b: 3:1, c: 4:1, d: 5:1) were 0.56 m^2/g, 0.32 m^2/g and 0.41 m^2/g, respectively. The surface morphology and specific surface area of the three proportions of PDA-CD polymer show little difference, which could explain that the true cross-linking ratio is not the added ratio, resulting in little difference between the three proportions of the polymer. It is further verified that PDA-CD retained the complete but

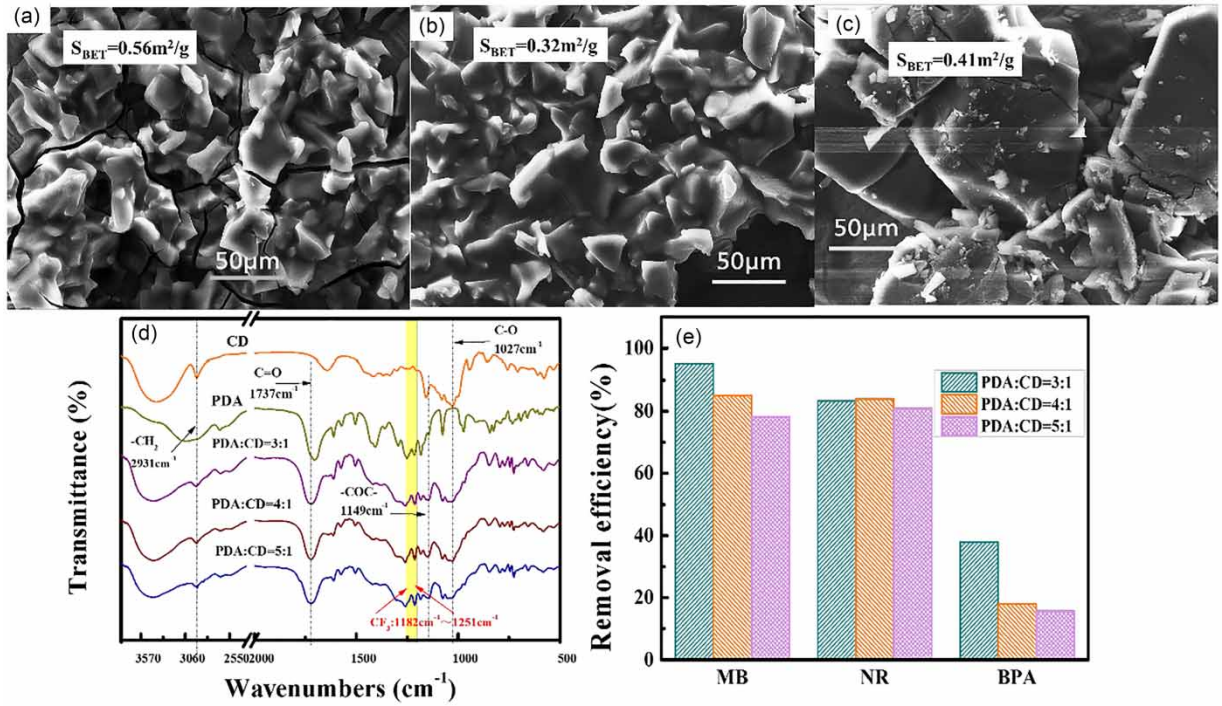

Figure 2 | The SEM image and BET data of PDA-CD polymers: (a) PDA:CD = 3:1; (b) PDA:CD = 4:1; (c) PDA:CD = 5:1. (d) The FT-IR spectra of CD and PDA-CD polymers with different ratios. (e) Adsorption of MB, NR and BPA by PDA-CD polymers with different molar ratios.

underdeveloped cavity structure of CD. Therefore, it is speculated that the adsorption capacities of the three ratios of polymer had great differences. Three pollutants (MB, NR and BPA) have been chosen to testify the adsorption properties of PDA-CD polymers. The relative results have been unfolded in Figure 2(e). When the PDA-CD were used in removal of MB, the removal efficiency with polymers in the ratio of 3:1 exceeded about 11% and 18%, in comparison with 4:1 and 5:1, respectively. For NR, the removal efficiency with polymers in three ratios were not too much different. Although the carboxyl groups on all three polymers were active, the amounts differ. Maybe their carboxyl groups were covered with different degrees. In addition, the dispersion of small particles in solution was good, but with the increase of the molar ratio of PDA/CD from 3 to 5, the dispersion of the polymer became worse, which was consistent with the results of SEM, resulting in less carboxyl group exposure. For BPA, polymers in the ratio of 3:1 had a great advantage that the removal efficiency exceeded about 52.6% and 58.4%, compared with the ratios of 4:1 and 5:1, respectively. Considering the result in BET, the oversupply of PDA would format self-polymerization to block the cavity of CD to different degrees. Thus, PDA-CD prepared in the ratio of 3:1 could retain as many carboxyl groups and cavities as possible.

Effect of pH on adsorption

The pH of solution has an important influence on the adsorption capacity. Zeta potential is used to investigate the surface charge of the adsorbent under different pH values and the results are shown in Figure 3(a). When the initial pH value of the solution was within 2.0–10.0, the Zeta potential of the polymers' surface was negative. It is explained that, in the aqueous environment, the -COOH on the surface of the PDA-CD tended to be deprotonated, resulting in $-COO^-$ groups and H^+ ions, contributing to the negatively charged surface of the polymers. With the pH values increased, the deprotonization of carboxyl groups was looming large. So that was why the Zeta potential nearly decreased all the time as the pH values increased. This case unquestionably has boosted formation of electrostatic attraction between polar pollutants and adsorbents. The result of the pH variation during the adsorption process is depicted in Figure 3(b), and this coincided with the variation trend of Zeta potentials. In the processes of adsorbing the MB and NR, the removal efficiencies had a close relationship with the pH of the initial solution. Combined with the experimental results in Figure 3(a), the Zeta potential of polymers showed a steep decrease. When the pH value was from 2.0 to 5.0, removal efficiencies of

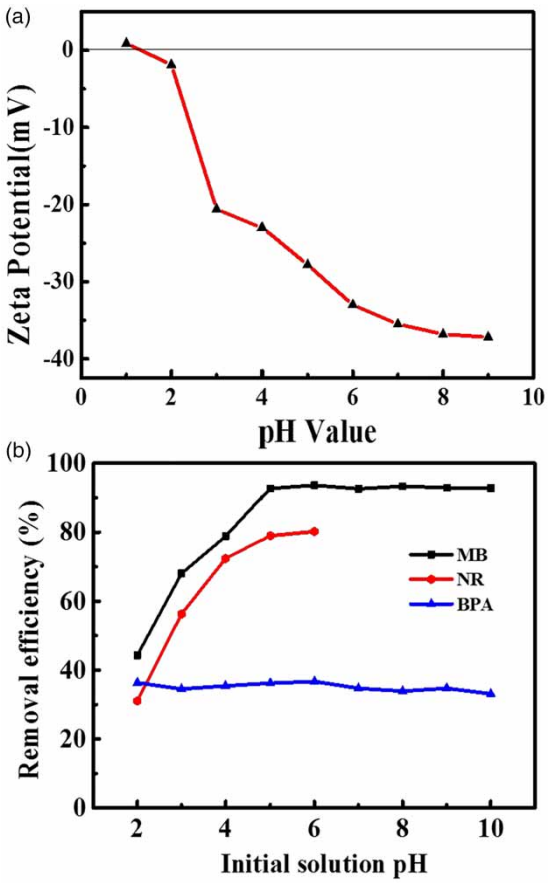

Figure 3 | (a) Effect of initial solution pH on the Zeta potentials of PDA-CD. Volume of deionized water: 10 mL, amount of polymers: 50 mg, temperature: 25 °C. (b) Effect of initial solution pH on the adsorption. Contaminant concentration: 50 mg/L, solution volume: 50 mL, adsorbent dosage: 1 g/L, temperature: 25 °C.

the MB and NR increased significantly from 44.3% to 92.7% and 31.1% to 80.2%, respectively. While the pH values were from 5.0 to 9.0, the Zeta potentials decreased slowly, but the corresponding removal efficiencies of dyes did not vary much. The differences in removal efficiency of dyes may arise from their different molecular shapes and pka values (Chen *et al.* 2020).

At low pH level, the protonation of functional groups in virtue of interacting with H^+ on PDA-CD contributes to the positive surface charge. The resulting repulsive forces suppressed the interaction of the cationic dyes on the adsorbent and the removal efficiency decreased. With pH value increased, the functional groups were more likely to deprotonate and the cationic dyes were favorably adsorbed by the negatively charged surface of PDA-CD (Zhou *et al.* 2019a). In contrast with MB and NR, the adsorption of BPA performed well over a broad range of pH values (2.0–10.0) and the removal efficiency stabilized in the range of 33% to 36%. This phenomenon is attributed to the cavity from CD forming host-guest compounds with BPA through hydrophobic interaction (Lee & Kwak 2019). Based on the analysis above, the pH of the solution was adjusted to 6.0 during the next experiments.

Adsorption isotherms

The isothermal adsorption on PDA-CD is exhibited in Figure 4(a)–4(c) and the parameters are demonstrated in Table 1. During the experiment, the initial pH of each pollutant solution was adjusted to 6.0.

The Langmuir model supposes one molecule in thickness and the adsorption sites on materials are assumed as identical and equivalent, without lateral interaction between the adsorbed molecules (Chen *et al.* 2020). Freundlich isotherm is used to describe non-ideal and reversible adsorption, not limited to monolayer adsorption. From Table 1, it can be found that all the parameters of $1/n_f$ are in the range between 0.1 and 0.5, indicating that all the adsorption processes of three pollutants belong to the favorable level (Crini 2008) and the relationship between the K_f values of the three pollutants follows as: K_f (MB) > K_f (NR) > K_f (BPA). It can be concluded that MB adsorption belonged to highest priority adsorption and BPA the lowest.

For the MB and NR in the three isothermal adsorption models, the correlation coefficient parameter (R^2) fitted by the Sips model was 0.961 and 0.950 respectively. The R^2 fitted by the Sips model is highest in comparison with the Langmuir and Freundlich models. The theoretical maximum dye (MB, NR) adsorption capacity (q_m) obtained by the Sips model can reach 113.06 mg/g and 106.8 mg/g, respectively, which is close to the experimental data (115.3 mg/g, 103.6 mg/g). For BPA, the Sips model also has the highest correlation coefficient of the three isothermal fitting models. The theoretical maximum BPA adsorption capacity (q_m) can reach 51.74 mg/g. Regarding the previous study of the adsorption of BPA by cyclodextrin polymer, it was concluded as a single-layer adsorption of pollutants in a 1:1 ratio, which fitted well with the Langmuir model (Wang & Harrison 2018; Lee & Kwak 2019). However, the Sips fitting model obtained in this paper is not contradictory to them. Considering the bias resulting from the transformation, the correlation coefficient may not the only consideration factor in judging the isotherm model (Foo & Hameed 2010). The Sips isotherm is a combination of the Langmuir and Freundlich models, which breaches the restriction of the potentially infinitive pollutants concentration in the Freundlich isotherm model (Meili *et al.* 2019).

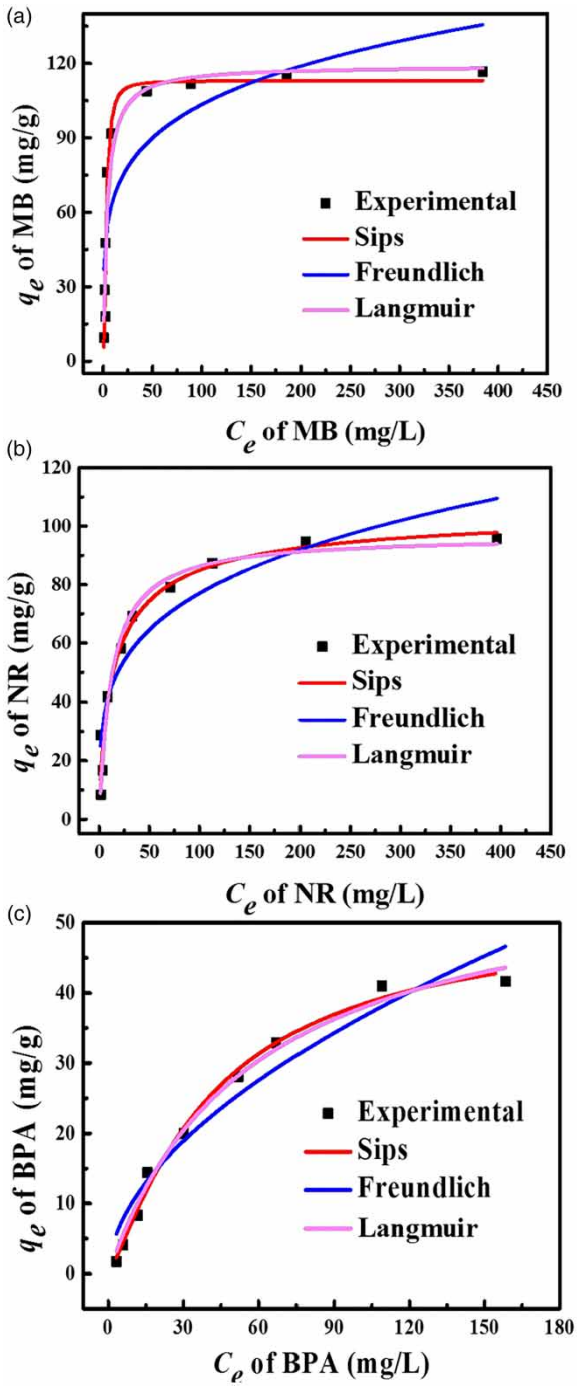

Figure 4 | Adsorption isotherms of pollutants by PDA-CD polymers (a: MB, b: NR, c: BPA) and model fitting.

Thus, the adsorption processes of dyes and BPA are detected as followed: diffused adsorption at low concentrations of pollutants and a monomolecular adsorption with a saturation value at high concentrations of pollutants (Muntean *et al.* 2013). According to *Ks* in Table 1, it can be inferred that MB has higher affinity than NR and BPA for the PDA-CD. The values of n_s in all pollutants adsorption are larger than 1, meaning that all processes are heterogeneous in nature. The data in Table 2 have shown some other materials to remove the MB, NR and BPA. By comparing $q_{e,max}$ of other materials, it can be found the adsorption capacity of our material is at high level. Furthermore, cyclodextrin adsorbents generally have a better ability to remove BPA.

Table 1 | Isothermal parameters of adsorption of MB, NR and BPA by PDA-CD

Isotherms	Parameters	Pollutants		
		MB	NR	BPA
Langmuir	q_m (mg/g)	119.10	96.81	59.44
	K_L (L/g)	0.2615	0.0816	0.0174
	R^2	0.9355	0.9445	0.9883
Freundlich	K_f ((g/kg)(g/m^3)^{nf})	41.02	23.80	2.99
	n_f	4.979	3.919	1.844
	R^2	0.7213	0.8725	0.9429
Sips	q_m (mg/g)	113.06	106.80	51.74
	K_S (L/g)	0.3231	0.0609	0.0238
	n_s	0.5618	1.334	0.832
	R^2	0.9610	0.9501	0.9901

Table 2 | Comparison of MB, NR and BPA adsorption capacity onto several adsorbents

Pollutants	Adsorbents	q_{max} (mg/g)	Reference
MB	DHHC	285.7	Simsek & Imamoglu (2015)
	SMSP	78.8	Senthamarai *et al.* (2013)
	BMHPs	264	Raza *et al.* (2019)
	HA1.0/CMC-3A	76.9	Chen *et al.* (2019)
	PDA-CD	113.1	This work
NR	TPC	114.9	Zou *et al.* (2012)
	$Ni_{0.5}Zn_{0.5}Fe_2O_4/SiO_2$	39.9	Liu *et al.* (2016b)
	CFY	113	Yuan *et al.* (2007)
	β-CDSP	29.5	Li *et al.* (2018)
	PDA-CD	106.8	This work
BPA	CA-*β*-CD	83.0	Huang *et al.* (2018)
	PAC	149.0	Ndagijimana *et al.* (2019)
	AC core 2	148.6	Ndagijimana *et al.* (2019)
	CSAC	28.5	Ndagijimana *et al.* (2019)
	Modified fibric peat	11.5	Zhou *et al.* (2011)
	BS-Mt	74.5	Liu *et al.* (2016a)
	SMNZ2	33.8	Li *et al.* (2014)
	PDA-CD	51.7	This work

Adsorption kinetics

As shown in Figure 5(a), when the effective contact time of MB reached 30 min, the equilibrium uptake achieved 80% and then achieved equilibrium within 180 min. For NR and BPA, the effective contact times were 40 min and 60 min, and the equilibrium adsorption capacity of PDA-CD can reach 39.91 mg/g and 18.35 mg/g after 180 min, respectively. The experimental results in Figure 5(a) also show that, after 30 min, the removal efficiency of MB, NR and BPA by PDA-CD can reach 80.9%, 57.9% and 22.4%, respectively.

In order to further explore the adsorption mechanism of PDA-CD in the adsorption process, pseudo-secondary dynamics models have been performed to fit with the experimental data of adsorption. The results in Figure 5(b) reveal that the kinetic data fitted well with the pseudo-second-order kinetic model, indicating that chemisorption dominates the entire processes of adsorption. Due to the data in Table 3, it can be found that the fitted adsorption capacity (q_e^{cal}) is close to the experimental results (q_e^{exp}). The k is usually used to estimate the rate of adsorption reaction. As shown in Table 3, the adsorption processes of MB, NR and BPA were all fast in the initial stage and then decelerated gradually along with the continuation of the reaction. Furthermore, the adsorption rate of PDA-CD for MB, NR and BPA is: MB > NR > BPA. This would be attributed to limited porosity making the cavity of CD less accessible to BPA comparing with the surface binding sites.

Table 3 | Kinetic parameters for adsorption of MB, NR and BPA by PDA-CD

Pollutant	Single/tandem system	q_e^{cal} (mg/g)	q_e^{exp} (mg/g)	$K*10^{-3}$ (g/mg/min)	R^2
MB	MB	48.54	47.04	3.823	0.9999
	NR/MB	35.97	34.17	3.476	0.9997
	BPA/MB	48.78	47.04	3.487	0.9999
	BPA/NR/MB	35.71	34.07	3.648	0.9997
	NR/BPA/MB	34.84	33.47	4.317	0.9998
NR	NR	42.55	39.91	1.889	0.9988
	MB/NR	28.57	26.93	2.952	0.9992
	BPA/NR	42.55	40.29	1.876	0.9991
	BPA/MB/NR	28.81	26.93	2.766	0.9994
	MB/BPA/NR	28.81	27.32	3.003	0.9985
BPA	BPA	21.27	18.35	1.799	0.9975
	MB/BPA	21.18	18.31	1.811	0.9980
	NR/BPA	21.27	18.23	1.799	0.9972
	MB/NR/BPA	21.09	18.14	1.797	0.9966
	NR/MB/BPA	21.14	18.25	1.811	0.9972

Tandem adsorption

As shown in Figure 5(c), the adsorption capacity of MB by PDA-CD can reach 47.04 mg/g in a single system after 180 min. After adsorption of BPA, the adsorption capacity

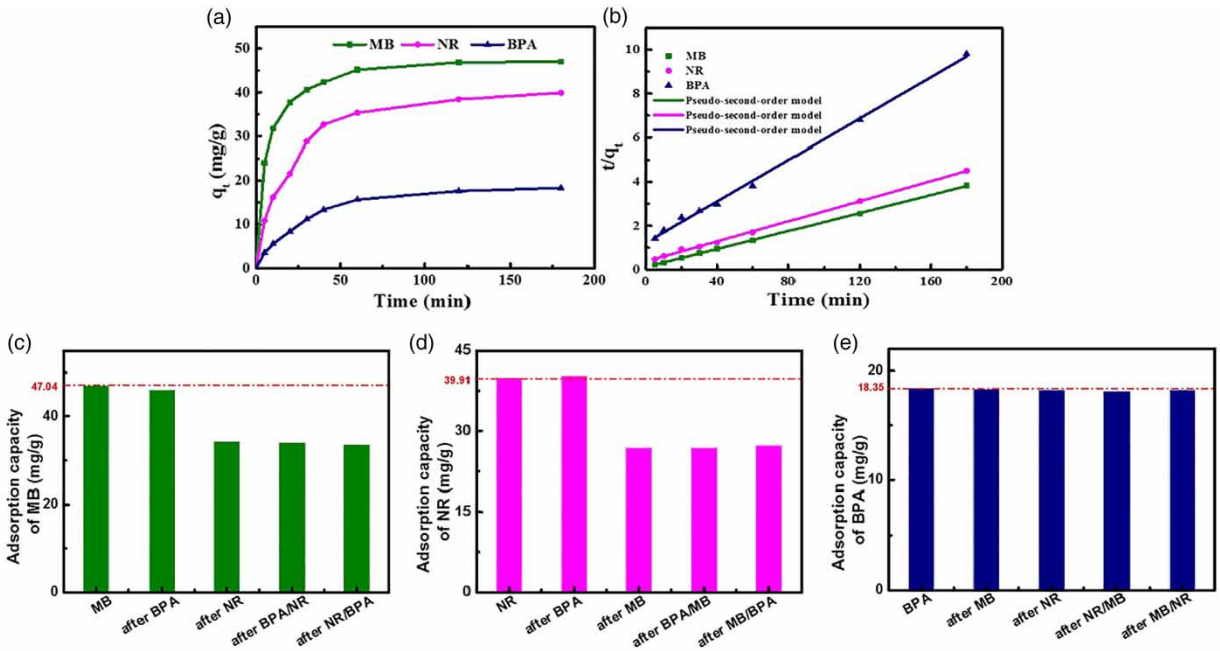

Figure 5 | Adsorption kinetics of MB, NR and BPA by PDA-CD polymers (a) and fitted by pseudo-second order kinetic model (b). The adsorption capacity (c) of MB after adsorption of NR, BPA, BPA/NR and NR/BPA after 180 min. The adsorption capacity (d) of NR after adsorption of MB, BPA, BPA/MB and MB/BPA after 180 min. The adsorption capacity (e) of BPA after adsorption of NR, MB, MB/NR and NR/MB after 180 min. Contaminant concentration: 50 mg/L, solution volume: 100 mL, adsorbent dosage: 1 g/L, initial pH: 6, temperature: 25 °C.

of MB changed little and maintained at about 47.04 mg/g. The adsorption kinetic curve in Figure 6(a) observed from the single system (MB) and dual system (BPA/MB) overlap almost completely. However, after adsorption of NR, the adsorption capacity of MB decreased to 34.17 mg/g. In two triple systems, MB adsorption capacities were all inhibited. After adsorption of NR/BPA and BPA/NR, the adsorption capacity of MB decreased by 26% and 28% to 33.47 mg/g and 34.07 mg/g, respectively. As shown in Figure 6(a), the trajectory of adsorption curves of dual (BPA/MB) is completely inconsistent with triple (NR/BPA/MB, BPA/NR/MB). It is proved that the adsorption processes of BPA and MB on PDA-CD are relative independently. However, NR on the adsorbent will inhibit the adsorption of MB.

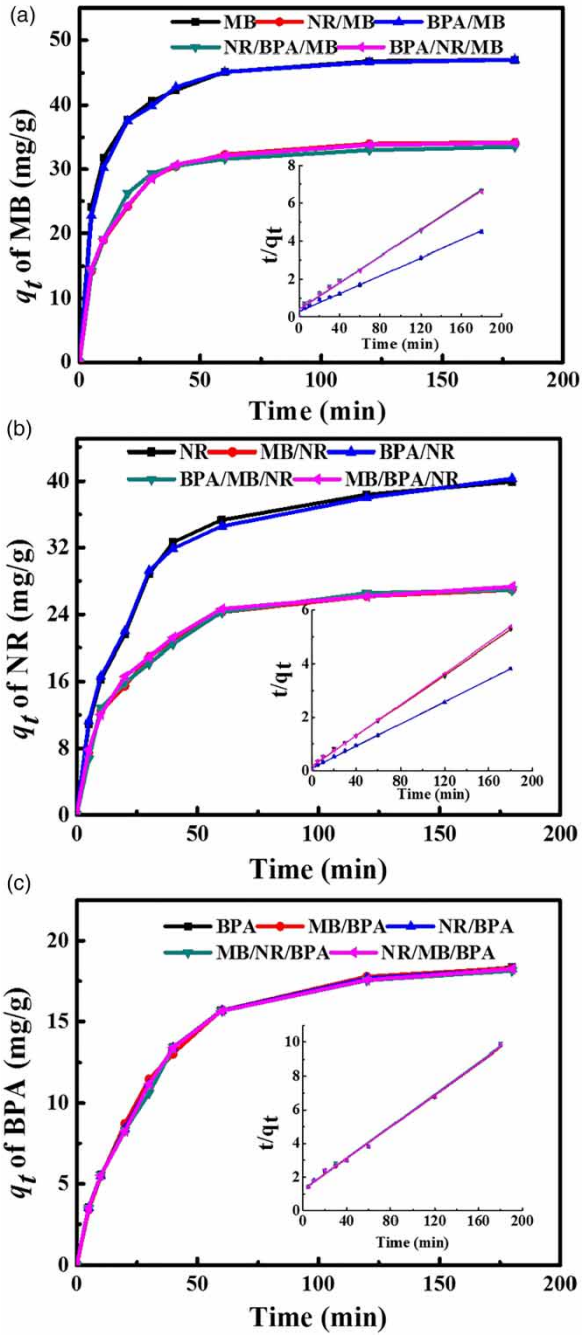

Figure 6 | Adsorption kinetics of MB (a), NR (b) and BPA (c) by PDA-CD polymers in the single and tandem system. Insets: adsorption kinetics fitted by pseudo-second order kinetic model. Contaminant concentration: 50 mg/L, solution volume: 100 mL, adsorbent dosage: 1 g/L, initial pH: 6, temperature: 25°C.

As shown in Figure 5(d), the adsorption capacity of NR by PDA-CD can reach 39.91 mg/g in the single system after 180 min. After adsorption of MB, MB/BPA and BPA/NR, the adsorption capacity of NR fell by 25%, 26% and 28% to 34.17, 33.47 and 34.07 mg/g, respectively. Figure 6(b) shows that the kinetic curves of MB/BPA/NR, BPA/MB/NR and MB/NR basically coincide, and completely disjunction with the kinetic curves of NR. However, BPA on the adsorbent did not affect the adsorption of MB, and its adsorption capacity was maintained at about 40.29 mg/g. The curve of BPA/NR in Figure 6(b) almost coincides with the kinetic curve of NR. MB on the adsorbent inhibited the adsorption of NR but did not affect the adsorption of BPA, which was consistent with the conclusion in Figure 5(c).

As shown in Figure 5(e), the adsorption capacity of BPA remained at about 18 mg/g in all four tandem systems, which was not significantly different from 18.34 mg/g in a single system. The five dynamics curves in Figure 6(c) almost coincide. This obviously shows that the adsorption of dye and BPA are two independent processes.

According to data in Table 3 and Figure 6, all the adsorption curves were in line with the pseudo-second-order kinetic model. This means that the dye or BPA on the adsorbent does not change the chemisorption-dominated processes.

It is well known that BPA is a kind of hydrophobic organic micro-pollutant. According to the 'internal hydrophobic, external hydrophilic' feature of cavity CD, BPA can be encapsulated by means of hydrophobic interactions (Kono *et al.* 2013; Huang *et al.* 2018; Zhou *et al.* 2019a). Numerous studies have proved that merely one phenyl ring of the BPA is able to get into the cavity of CD, while the other stayed outside (Yang *et al.* 2008). Weiwei Huang *et al.* (Huang *et al.* 2018) argued that coexistence of two or more pollutants in one CD cavity was impossible because of the molecular structure. Meanwhile, the BET characterization indicates that the pore structure of the PDA-CD is underdeveloped and the cyclodextrin cavity provides less

adsorption sites than the sites provided by the carboxyl group on the surface. The results of the researches above have further determined our hypothesis that adsorptions of dyes and BPA are mainly attributed to carboxyl groups on PDA and the hydrophobic cavity in CD, respectively.

Effect of fulvic acid and inorganic ion

In total, 3–28% of the organic matter in sewage is humus (Moura *et al.* 2007). The choice of FA is because it is the most soluble and mobile component of humus in water and would interfere with the adsorbent relying on its rich groups (Yang & Xing 2009). Therefore, in order to study the stability and anti-interference ability of PDA-CD, this section selected FA as a representative of natural organic matter to study the adsorption of natural organic matter on PDA-CD. The relative experimental results are shown in Figure 7(a).

The experimental results show that when the concentration of FA in the solution was in the range of 20 mg/L to 200 mg/L, the removal efficiencies of the three target pollutants (MB, NR, BPA) remained basically alike. The removal efficiencies of MB, NR and BPA were maintained in the range of 92.3% to 93.7%, 79.2% to 80.3%, and 34.7% to 36.7%, respectively. These results indicate that the PDA-CD has superior anti-interference ability and practical application potential. There are two main reasons for this: firstly, the previous analysis and proof that MB and NR were removed from the aqueous solution by binding to the carboxyl group on the surface of the PDA-CD adsorbent material. However, FA did not react with carboxyl groups, and the presence of FA in the solution did not affect the adsorption of MB and NR; secondly, the FA molecule has a large size and cannot enter the hydrophobic cyclodextrin cavity, thus it would not compete with BPA for adsorption sites in the solution. So it can be concluded that the presence of FA in the solution will not affect the PDA-CD adsorption of BPA. In addition to humic acid, there are other complex organic compounds in the textile effluents. The specific organic composition depends on the printing and dyeing process and the type of additives added.

On the other hand, considering various inorganic ions such as K^+, Ca^{2+} and Cl^- exist in actual textile wastewater, the effect of mineral ions needs to be analyzed. These ions may compete with the contaminant molecules for the adsorption sites available on the adsorbent, resulting in a decrease in the adsorption performance of the adsorbent. As seen from Figure 7(b), when the K^+ ion concentration in the solution was 20 mg/L or 200 mg/L, the adsorption capacity of PDA-CD for MB, NR and BPA did not differ much compared with previously.

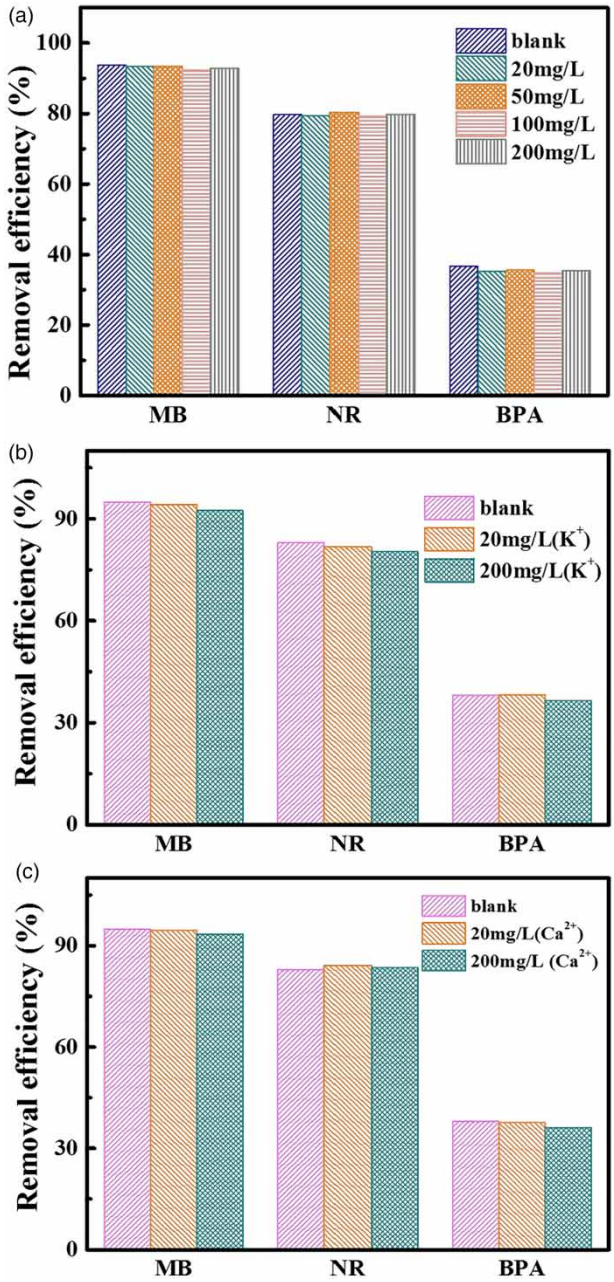

Figure 7 | Effect of concentrations of coexisting FA (a), Ca^{2+} (b) and K^+ (c) on the removal efficiencies of MB, NR and BPA. Solution volume: 50 mL, adsorbent dosage: 1 g/L, contaminant concentration: 50 mg/L, temperature: 25 °C, initial pH: 6.0.

The removal efficiencies of MB in two concentrations of K^+ ion were 94.2% (20 mg/L) and 92.3% (200 mg/L), and NR were 81.6% (20 mg/L) and 80.4% (200 mg/L). The removal efficiencies of BPA were 38.2% (20 mg/L) and 36.4% (200 mg/L). Compared with the blank experiment

data, the adsorption capacity did not present too much difference. Similarly, when 20 mg/L and 200 mg/L of Ca^{2+} ions were present in solution, shown in Figure 7(c), the removal efficiencies of the three contaminants in the solution were hardly affected. Such results indicate that the adsorption performances of the adsorbent PDA-CD to MB, NR and BPA were hardly affected while the inorganic ions existed in the solution.

Proposed adsorption mechanism

For gaining insight into the adsorption mechanism of adsorption performances, the FT-IR before and after adsorption needs to be compared. The results are presented in Figure 8. It was found that the phenolic O-H absorption peak of PDA-CD shifted ($3{,}419\ cm^{-1} \rightarrow 3{,}437\ cm^{-1}$) after adsorbing BPA. It can be reasonably inferred that BPA adsorbed on PDA-CD caused the shift of the phenolic O-H absorption peak. At the same time, the intensity of the C = O ($1{,}737\ cm^{-1}$) absorption peak on the adsorbed PDA-CD-NR and PDA-CD-MB is weaker than that of PDA-CD, which can predict that the NR molecules and the MB molecules indeed interacted with -COOH on the PDA-CD via electrostatic attraction. Li *et al.* (2018) concluded that π–π interactions with the benzene rings on β-CDSP and adsorbates contributed significantly to the adsorption of NR. Fu *et al.* (2015) pointed that the π–π stacking interactions could occur between MB molecules and dopamine according to MB is an ideally planar molecule with abundant aromatic rings. Liu *et al.* (2019) have achieved a similar conclusion. It is noticed that MB and NR are planar molecules with abundant aromatic rings and a PDA molecule also has two benzene rings. Due to the results in Figure 8, the stretching vibration band of C = C on the aromatic ring is obviously shifted after the dyes were adsorbed (MB:$1{,}612\ cm^{-1} \rightarrow 1{,}621\ cm^{-1}$, NR:$1{,}612\ cm^{-1} \rightarrow 1{,}596\ cm^{-1}$). So it can be confirmed that π–π stacking interactions can happen between MB molecules and PDA-CD, resulting in the shift of the peak.

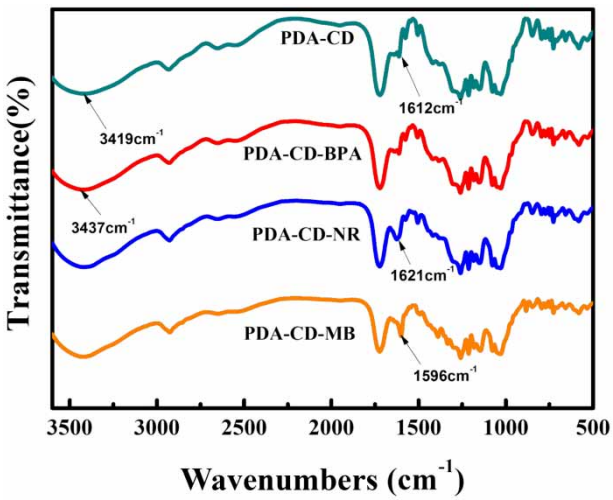

Figure 8 | FT-IR spectra of PDA-CD polymers before and after MB, NR and BPA adsorption.

CONCLUSION

In this paper, CD, a kind of oligosaccharide extracted from starch-containing crops, was cross-linked with PDA in three different molar ratios (PDA: CD = 3:1, PDA: CD = 4:1, PDA: CD = 5:1) through simple and friendly synthesis procedures. The molar ratio of 3:1 (PDA: CD = 3:1) was the most optimal choice by comparing yields, water absorption volumes and adsorption performances. The PDA-CD showed good adsorption performances in an extensive pH range of 4.0 to 10.0. Besides, the kinetics and isotherms studies showed that the adsorption processes abided by the pseudo-second-order kinetic model and the Sips model, respectively. The maximum adsorption capacities can reach 51.74 mg/g for BPA, 113.06 mg/g for MB and 106.8 mg/g for NR. Through tandem adsorption, it is further proved that the adsorption processes of dyes and BPA are relatively independent. Moreover, PDA-CD had a strong anti-interference ability. The FA and inorganic ions (K^+, Ca^{2+}) had little effect on the adsorption performance. Considering the actual situation of textile wastewaters, this kind of polymer will be a good choice for treatment in the future.

FUNDING INFORMATION

This work was supported by the National Natural Science Foundation of China (51778230), Shanghai Rising-Star Program (17QA1401000), and the Fundamental Research Funds for the Central Universities for their financial support (222201718003).

REFERENCES

Acemioglu, B. 2005 Batch kinetic study of sorption of methylene blue by perlite. *Chemical Engineering Journal* **106** (1), 73–81.

Chen, W., Lin, Q., Cheng, S., Wu, M., Tian, Y., Ni, K., Bai, Y. & Ma, H. 2019 Synthesis and adsorption properties of

amphoteric adsorbent HAx/CMC-yAl. *Separation and Purification Technology* **221**, 338–348.

Chen, H., Zhou, Y., Wang, J., Lu, J. & Zhou, Y. 2020 Polydopamine modified cyclodextrin polymer as efficient adsorbent for removing cationic dyes and Cu^{2+}. *Journal of Hazardous Materials* **389**, 121897.

Choi, Y., Sinha, A., Im, J., Jung, H. & Kim, J. 2019 Hierarchically porous composite scaffold composed of SBA-15 microrods and reduced graphene oxide functionalized with cyclodextrin for water purification. *ACS Applied Materials & Interfaces* **11** (17), 15764–15772.

Crini, G. 2008 Kinetic and equilibrium studies on the removal of cationic dyes from aqueous solution by adsorption onto a cyclodextrin polymer. *Dyes and Pigments* **77** (2), 415–426.

Crini, G. 2014 Review: a history of cyclodextrins. *Chemical Reviews* **114** (21), 10940–10975.

Foo, K. Y. & Hameed, B. H. 2010 Insights into the modeling of adsorption isotherm systems. *Chemical Engineering Journal* **156** (1), 2–10.

Fu, J., Chen, Z., Wang, M., Liu, S., Zhang, J., Zhang, J., Han, R. & Xu, Q. 2015 Adsorption of methylene blue by a high-efficiency adsorbent (polydopamine microspheres): kinetics, isotherm, thermodynamics and mechanism analysis. *Chemical Engineering Journal* **259**, 53–61.

Gamoudi, S. & Srasra, E. 2019 Adsorption of organic dyes by $HDPy^{+}$-modified clay: effect of molecular structure on the adsorption. *Journal of Molecular Structure* **1193**, 522–531.

Guo, L. M., Yang, Y. Z. & Wang, Y. 2019 Single-step coating of polyethylenimine on gradient nanoporous phenolics for tight membranes with ultrahigh permeance. *Journal of Membrane Science* **587**, 117172.

Hu, X., Xu, G., Zhang, H., Li, M., Tu, Y., Xie, X., Zhu, Y., Jiang, L., Zhu, X., Ji, X., Li, Y. & Li, A. 2020 Multifunctional β-cyclodextrin polymer for simultaneous removal of natural organic matter and organic micropollutants and detrimental microorganisms from water. *ACS Applied Materials & Interfaces* **12** (10), 12165–12175.

Huang, W., Hu, Y., Li, Y., Zhou, Y., Niu, D., Lei, Z. & Zhang, Z. 2018 Citric acid-crosslinked β-cyclodextrin for simultaneous removal of bisphenol A, methylene blue and copper: the roles of cavity and surface functional groups. *Journal of the Taiwan Institute of Chemical Engineers* **82**, 189–197.

Kloster, G. A., Mosiewicki, M. A. & Marcovich, N. E. 2019 Chitosan/iron oxide nanocomposite films: effect of the composition and preparation methods on the adsorption of Congo red. *Carbohydrate Polymers* **221**, 186–194.

Konca, K. & Çulfaz-Emecen, P. Z. 2019 Effect of carboxylic acid crosslinking of cellulose membranes on nanofiltration performance in ethanol and dimethylsulfoxide. *Journal of Membrane Science* **587**, 117175.

Kono, H., Onishi, K. & Nakamura, T. 2013 Characterization and bisphenol A adsorption capacity of β-cyclodextrin–carboxymethylcellulose-based hydrogels. *Carbohydrate Polymers* **98** (1), 784–792.

Lee, J. H. & Kwak, S.-Y. 2019 Rapid adsorption of bisphenol A from wastewater by β-cyclodextrin-functionalized mesoporous magnetic clusters. *Applied Surface Science* **467–468**, 178–184.

Li, J., Zhan, Y., Lin, J., Jiang, A. & Xi, W. 2014 Removal of bisphenol A from aqueous solution using cetylpyridinium bromide (CPB)-modified natural zeolites as adsorbents. *Environmental Earth Sciences* **72** (10), 3969–3980.

Li, X., Xie, L., Yang, X. & Nie, X. 2018 Adsorption behavior and mechanism of β-cyclodextrin-styrene-based polymer for cationic dyes. *RSC Advances* **8** (70), 40321–9.

Liu, L., Gao, Z. Y., Su, X. P., Chen, X., Jiang, L. & Yao, J. M. 2015 Adsorption removal of dyes from single and binary solutions using a cellulose-based bioadsorbent. *ACS Sustainable Chemistry and Engineering* **3** (3), 432–442.

Liu, C., Wu, P., Zhu, Y. & Tran, L. 2016a Simultaneous adsorption of Cd^{2+} and BPA on amphoteric surfactant activated montmorillonite. *Chemosphere* **144**, 1026–1032.

Liu, R. J., Fu, H. X., Lu, Y. M., Yin, H. Q., Yu, L. Q., Ma, L. Y. & Han, J. 2016b Adsorption optimization and mechanism of neutral red onto magnetic $Ni_{0.5}Zn_{0.5}Fe_2O_4/SiO_2$ nanocomposites. *Journal of Nanoscience and Nanotechnology* **16** (8), 8252–8262.

Liu, D., Huang, Z., Li, M., Sun, P., Yu, T. & Zhou, L. 2019 Novel porous magnetic nanospheres functionalized by β-cyclodextrin polymer and its application in organic pollutants from aqueous solution. *Environmental Pollution* **250**, 639–649.

Liu, Q., Li, Y., Chen, H., Lu, J., Yu, G., Möslang, M. & Zhou, Y. 2020 Superior adsorption capacity of functionalised straw adsorbent for dyes and heavy-metal ions. *Journal of Hazardous Materials* **382**, 121040.

Meili, L., Lins, P. V. S., Costa, M. T., Almeida, R. L., Abud, A. K. S., Soletti, J. I., Dotto, G. L., Tanabe, E. H., Sellaoui, L., Carvalho, S. H. V. & Erto, A. 2019 Adsorption of methylene blue on agroindustrial wastes: experimental investigation and phenomenological modelling. *Progress in Biophysics and Molecular Biology* **141**, 60–71.

Moura, M. N., Martín, M. J. & Burguillo, F. J. 2007 A comparative study of the adsorption of humic acid, fulvic acid and phenol onto Bacillus subtilis and activated sludge. *Journal of Hazardous Materials* **149** (1), 42–48.

Muntean, S. G., Paska, O., Coseri, S., Simu, G. M., Grad, M. E. & Ilia, G. 2013 Evaluation of a functionalized copolymer as adsorbent on direct dyes removal process: kinetics and equilibrium studies. *Journal of Applied Polymer Science* **127** (6), 4409–4421.

Ndagijimana, P., Liu, X., Li, Z., Yu, G. & Wang, Y. 2019 Optimized synthesis of a core-shell structure activated carbon and its adsorption performance for Bisphenol A. *Science of The Total Environment* **689**, 457–468.

Ozmen, E. Y., Sezgin, M., Yilmaz, A. & Yilmaz, M. 2008 Synthesis of β-cyclodextrin and starch based polymers for sorption of azo dyes from aqueous solutions. *Bioresource Technology* **99** (3), 526–531.

Qadeer, R. 2007 Adsorption behavior of ruthenium ions on activated charcoal from nirtic acid medium. *Colloids and Surfaces A: Physicochemical and Engineering Aspects* **293** (1–3), 217–223.

Raza, S., Yong, X. & Deng, J. 2019 Immobilizing cellulase on multi-layered magnetic hollow particles: preparation, bio-catalysis and adsorption performances. *Microporous and Mesoporous Materials* **285**, 112–119.

Ren, L., Fu, W., Luo, Y., Lu, H., Jia, D., Shen, J., Pang, B. & Ko, T.-M. 2004 Thermal degradation of the polyimide synthesized from 4,4′-(hexafluoroisopropylidene)diphthalic dianhydride and 4,4′-diaminodiphenylmethane. *Journal of Applied Polymer Science* **91** (4), 2295–2301.

Robinson, T., McMullan, G., Marchant, R. & Nigam, P. 2001 Remediation of dyes in textile effluent: a critical review on current treatment technologies with a proposed alternative. *Bioresource Technology* **77** (3), 247–255.

Senthamarai, C., Kumar, P. S., Priyadharshini, M., Vijayalakshmi, P., Kumar, V. V., Baskaralingam, P., Thiruvengadaravi, K. V. & Sivanesan, S. 2013 Adsorption behavior of methylene blue dye onto surface modified *Strychnos potatorum* seeds. *Environmental Progress & Sustainable Energy* **32** (3), 624–632.

Simsek, G. & Imamoglu, M. 2015 Investigation of equilibrium, kinetic and thermodynamic of methylene blue adsorption onto dehydrated hazelnut husk carbon. *Desalination and Water Treatment* **54** (6), 1747–1753.

Van, H. T., Nguyen, L. H., Hoang, T. K., Tran, T. P., Vo, A. T., Pham, T. T. & Nguyen, X. C. 2019 Using FeO-constituted iron slag wastes as heterogeneous catalyst for Fenton and ozonation processes to degrade Reactive Red 24 from aqueous solution. *Separation and Purification Technology* **224**, 431–442.

Verma, A. K., Dash, R. R. & Bhunia, P. 2012 A review on chemical coagulation/flocculation technologies for removal of colour from textile wastewaters. *Journal of Environmental Management* **93** (1), 154–168.

Wang, J. Z. & Harrison, M. 2018 Removal of organic micro-pollutants from water by -cyclodextrin triazine polymers. *Journal of Inclusion Phenomena and Macrocyclic Chemistry* **92** (3–4), 347–356.

Wu, D., Hu, L., Wang, Y., Wei, Q., Yan, L., Yan, T., Li, Y. & Du, B. 2018 EDTA modified β-cyclodextrin/chitosan for rapid removal of Pb(II) and acid red from aqueous solution. *Journal of Colloid and Interface Science* **523**, 56–64.

Xu, H., Zhou, C., Jian, C., Yang, S., Liu, M., Huang, X., Gao, W. & Wu, H. 2020 Salt/current-triggered stabilization of β-cyclodextrins encapsulated host-guest low-molecular-weight gels. *Chinese Chemical Letters* **31** (2), 369–372.

Xue, J., Liu, W. & Kannan, K. 2017 Bisphenols, benzophenones, and bisphenol A diglycidyl ethers in textiles and infant clothing. *Environmental Science & Technology* **51** (9), 5279–5286.

Yang, K. & Xing, B. 2009 Adsorption of fulvic acid by carbon nanotubes from water. *Environmental Pollution* **157** (4), 1095–1100.

Yang, Z. X., Chen, Y. & Liu, Y. 2008 Inclusion complexes of bisphenol A with cyclomaltoheptaose (β-cyclodextrin): solubilization and structure. *Carbohydrate Research* **343** (14), 2439–2442.

Yang, Q., Wang, B., Chen, Y., Xie, Y. & Li, J. 2019 An anionic In(III)-based metal-organic framework with Lewis basic sites for the selective adsorption and separation of organic cationic dyes. *Chinese Chemical Letters* **30** (1), 234–238.

Yuan, X., Zhuo, S.-P., Xing, W., Cui, H.-Y., Dai, X.-D., Liu, X.-M. & Yan, Z.-F. 2007 Aqueous dye adsorption on ordered mesoporous carbons. *Journal of Colloid and Interface Science* **310** (1), 83–89.

Zhang, M., Zhu, L., He, C., Xu, X., Duan, Z., Liu, S., Song, M., Song, S., Shi, J., Li, Y. e. & Cao, G. 2019 Adsorption performance and mechanisms of Pb(II), Cd(II), and Mn(II) removal by a β-cyclodextrin derivative. *Environmental Science and Pollution Research* **26** (5), 5094–5110.

Zhao, D., Zhao, L., Zhu, C. S., Shen, X., Zhang, X. & Sha, B. 2009 Comparative study of polymer containing β-cyclodextrin and -COOH for adsorption toward aniline, 1-naphthylamine and methylene blue. *Journal of Hazardous Materials* **171** (1–3), 241–246.

Zhao, F., Repo, E., Yin, D., Meng, Y., Jafari, S. & Sillanpää, M. 2015 EDTA-cross-linked β-cyclodextrin: an environmentally friendly bifunctional adsorbent for simultaneous adsorption of metals and cationic dyes. *Environmental Science & Technology* **49** (17), 10570–10580.

Zhou, Y., Chen, L., Lu, P., Tang, X. & Lu, J. 2011 Removal of bisphenol A from aqueous solution using modified fibric peat as a novel biosorbent. *Separation and Purification Technology* **81** (2), 184–190.

Zhou, Y., Cheng, G., Chen, K., Lu, J., Lei, J. & Pu, S. 2019a Adsorptive removal of bisphenol A, chloroxylenol, and carbamazepine from water using a novel β-cyclodextrin polymer. *Ecotoxicology and Environmental Safety* **170**, 278–285.

Zhou, Y., Lu, J., Zhou, Y. & Liu, Y. 2019b Recent advances for dyes removal using novel adsorbents: a review. *Environmental Pollution* **252**, 352–365.

Zhou, Y., He, J., Lu, J., Liu, Y. & Zhou, Y. 2020 Enhanced removal of bisphenol A by cyclodextrin in photocatalytic systems: degradation intermediates and toxicity evaluation. *Chinese Chemical Letters*. https://doi.org/10.1016/j.cclet.2020.02.008.

Zijian, Z., Qingwei, G., Zhencheng, X., Li, W. & Kai, C. 2015 Distribution and removal of endocrine-disrupting chemicals in industrial wastewater treatment. *Environmental Engineering Science* **32** (3), 203–211.

Zou, W., Bai, H. & Gao, S. 2012 Competitive adsorption of neutral Red and Cu^{2+} onto pyrolytic char: isotherm and kinetic study. *Journal of Chemical & Engineering Data* **57** (10), 2792–2801.

First received 10 January 2020; accepted in revised form 2 June 2020. Available online 15 June 2020